https://doi.org/10.22320/s0718221x/2024.11

ARTÍCULO

Performance of visible and Near-infrared spectroscopy to predict the energetic properties of wood

Franciele Gmach[1] https://orcid.org/0000-0002-7097-6813
Letícia Jacobowski Arruda[2] https://orcid.org/0009-0004-8406-1595
Eraldo Antonio Bonfatti Júnior[1♠] https://orcid.org/0000-0002-2730-7681
Elaine Cristina Lengoeski[3] https://orcid.org/0000-0002-7336-7626
Rudson Silva Oliveira[1] https://orcid.org/0000-0002-9659-9331
Dimas Agostinho da Silva[1] https://orcid.org/0000-0002-5433-1927
Silvana Nisgoski[1] https://orcid.org/0000-0001-9595-9131
Lívia Cássia Viana[4] https://orcid.org/0000-0001-8020-2478
Diego Martins Stangerlin[3] https://orcid.org/0000-0003-4336-6793

[1]Federal University of Paraná. Paraná, Brazil
[2]Universidade do Contestado, Santa Catarina, Brazil
[3]Universidade Federal de Mato Grosso. Mato Grosso, Brazil
[4]Federal University of Tocantins. Tocantins, Brazil

[♠]Corresponding author: bonfattieraldo@gmail.com

Abstract:
Wood can be used for fuel by direct burning, or as a raw material for other fuels; however, it is necessary to evaluate the energy properties to ensure the optimal use of this material. The most relevant characteristics to be analyzed are the higher heating value, volatile material content, fixed carbon content, and ash content. Along with the traditional methods, there are also non-destructive evaluations that are optimized for speed and reliability. Among these methods, visible spectroscopy and near-infrared spectroscopy have been proven to be robust for the prediction of several wood properties. The aim of this study was to evaluate the potential of visible spectroscopy and near-infrared spectroscopy for species discrimination and prediction of higher heating value, volatile material content, fixed carbon content, and ash content for *Eucalyptus saligna*, *Eucalyptus dunnii*, and *Eucalyptus benthamii* woods. For this purpose, multivariate principal component analysis and partial least squares regression were applied to the collected spectra. The principal component analysis satisfactorily discriminated the three species, explaining 99% of the variance of the visible spectroscopy spectra and 73% of that of the near-infrared spectra. The estimation of energetic properties through partial least squares regression was satisfactory for both visible spectroscopy and near-infrared spectroscopies, which presented calibration R^2 values close to 1 and low errors for all properties studied.

Keywords: Biofuel, chemometrics, *Eucalyptus,* heating value, multivariate analysis, Near-infrared spectroscopy.

Received: 24.01.2022
Accepted: 02.11.2023
Posted online: 02.11.2023

Introduction

Wood can be used for energy production in the form of firewood, charcoal formed by the pyrolysis process that is compacted into pellets or briquettes, or sawdust and wood chips, which are wood wastes that are mechanically burned. It also serves as a raw material to produce biofuels from gasification, liquefaction, and fermentation processes. This versatility, added to the natural origin of wood, makes its use for energy purposes evident (Oliveira *et al.* 2016). However, along with burning and taking advantage of the heat released, the proper characterization of its energy properties, using such factors as the heating value and proximate analysis, is necessary to ensure the optimal use of this material as fuel (Costa Junior *et al.* 2021).

The heating value (HV) is the amount of heat released in the complete burning of one unit mass of a fuel (PincellI and Queiroz 2021). This is expressed as the ratio between the unit of energy and the unit of mass (Friedl *et al.* 2005, Bersch *et al.* 2018), and can be classified as a lower heating value (LHV) or a higher heating value (HHV) (Cortez *et al.* 2014). LHV is the energy effectively available per unit mass of fuel after deducting losses from water evaporation, while HHV is the amount of heat released during combustion with water in condensed form (Cortez *et al.* 2014).

The proximate analysis of fuels involves the determination of the volatile material content, ash content, and fixed carbon content (Lana *et al.* 2016, Loureiro *et al.* 2021). Knowledge of these three properties is fundamental for the control of processes that use wood fuels, and together with the heating value, they are the most used energy characteristics for lignocellulosic biomass evaluation (Friedl *et al.* 2005).

The volatile material content (VMC) is the part of the wood that evaporates at the beginning of the heating process, including water (McKendry 2002). A higher VMC may indicate rapid ignition, but it decreases the residence time of the fuel inside the thermal machine, causing low energy efficiency (McKendry 2002, Cortez *et al.* 2014).

Ashes are a heterogeneous set of oxides (Garcia-Maraver *et al.* 2017) that are formed during combustion by the oxidation of inorganic components present in wood (Vassilev and Vassileva 2020). The ash content (AC) is the most undesirable property from an energy point of view (Bonfatti Júnior *et al.* 2019), since besides not generating heat, it is the main impurity of fuels which causes abrasions to the metallic components of thermal machines (Liu *et al.* 2014).

The fixed carbon content (FCC) is inversely proportional to the volatile material and ash contents (Orellana *et al.* 2020), since along with ash, it is the remaining mass after the release of volatile materials (McKendry 2002). This property is associated with the HHV of lignocellulosic biomass (Garcia-Maraver *et al.* 2017). Therefore, when wood is considered for energy purposes, it is desirable for it to have a high fixed carbon content.

Wood is a heterogeneous material formed by natural polymers, such as lignin, cellulose, and hemicelluloses, as well as low molecular weight substances called extractives. The proportions of these chemical components vary between species, individual trees, and even within the tree stem. The energetic properties of wood are related to its chemical composition; however, despite possible variations in chemistry, the energetic properties of this material have typical values. On average, most wood has a VMC between 70 and 87%, FCC between 15 and 30%, AC not exceeding 1% (Shen *et al.* 2010), and an HHV of approximately 4500 kcal kg^{-1} (Telmo and Lousada 2011).

Non-destructive techniques identify the properties and characteristics of materials without impairing their usability (Pádua *et al.* 2019) using highly efficient tests (Llana *et*

al. 2020). Considering that the energy characterization of lignocellulosic biomass is time-consuming, costly, and destructive, the application of non-destructive techniques may facilitate the evaluation of the wood as a potential biofuel.

Non-destructive techniques include visible spectroscopy (VIS) and near-infrared spectroscopy (NIRS). These methods obtain spectra and correlate them with the results of destructive analysis to generate a statistical model that explains and correlates most of the information contained in the spectra (Amaral *et al.* 2020) using multivariate calibration (Cunha *et al.* 2020). Within the electromagnetic spectrum, NIRS measures the intensity of absorbance or reflectance of near-infrared radiation, with wavelengths in the range of 780-2500 nm, whereas VIS determines these intensities in the visible range of 400-700 nm (Rumble 2020).

VIS and NIRS are suitable techniques to replace laborious and uneconomic conventional analyses, as they require no treatment of the sample, are rapid and readily assessed, and have the potential for automation and on-site application (Casson *et al.* 2020, Santos *et al.* 2021). In wood science, these techniques have proven useful in predicting chemical properties (Lengowski *et al.* 2018), moisture content (Kobori *et al.* 2013, Chen and Li 2020), basic density (Li *et al.* 2020, de Abreu Neto *et al.* 2020), anatomical element sizes (Li *et al.* 2018) and mechanical properties (Kobori *et al.* 2013, de Abreu Neto *et al.* 2020), as well as for identifying species (Nisgoski *et al.* 2017). In the energy context, they are feasible for the assessment of biodiesel quality (Pilar Dorado *et al.* 2011, Fernandes *et al.* 2011), prediction of the heating value of manure (Preece *et al.* 2013), and rapid determination of total petroleum hydrocarbon content (Douglas *et al.* 2018).

The aim of this study was to evaluate the potential of VIS and NIRS for species discrimination, and to predict the HHV and proximate analysis of wood using multivariate calibration techniques such as principal component analysis (PCA) and

partial least squares regression (PLS-R). The wood from three eucalyptus species was used for these assessments.

Material and methods

Wood

The present study used wood from *Eucalyptus benthamii* Maiden & Cambage, *Eucalyptus dunnii* Maiden, *Eucalyptus saligna* Sm grown in a 6-year-old experimental forest in Canoinhas city, Santa Catarina state, Brazil. Nine trees per species were selected, considering the average stem diameter at breast height (DBH). Disks were removed from these trees at 0 %, 25 %, 50 %, 75 %, and 100 % of the commercial stem height, and two opposite wedges were removed from each disk. These wedges were reduced to sawdust in accordance with the TAPPI T257 sp-21 (2021) and then mixed to form a composite sample with the wood from the five heights collected.

In total, nine samples of sawdust per species (one per tree) were produced and used for the analysis of energy properties and for the collection of spectra in the NIR and VIS regions.

Determination of wood energy properties

The HHV was determined according to the standard ASTM D5865-13 (2013) in an IKA C-5000 automated bomb calorimeter (IKA, Staufen, Germany). The VMC, AC, and FCC were determined according to the standards ASTM E872-82 (2019), ASTM D1102-84 (2021), and ASTM E870-82 (2019), respectively.

All these analyses were conducted in triplicate, and the statistical evaluation was performed using the Grubbs test for outliers, Shapiro-Wilk test for data normality, Levene test for homogeneity of variance, and analysis of variance (ANOVA). The Tukey mean comparison test was performed when the equality hypothesis was rejected. All tests were performed using the Statgraphics Centurion XV program (Statgraphics Technologies, Inc., Virginia, United States) at a 5% probability.

Obtaining the spectra

The spectra were collected from the wood sawdust at a temperature of 23 ± 2 °C and a relative humidity of 60 %, with 45 repetitions for each species for a total of 135 spectra. To obtain the spectra in VIS light, a Konica Minolta CM-5 spectrophotometer (Konica Minolta, Ramsey, USA) coupled to a computer with an adjustment for the D65 light source and a 10º observation angle was used. The data were collected in reflectance mode, with a spectral range of 400-750 nm.

NIR spectroscopy was performed using a Bruker Tensor 37 spectrometer (Bruker Optics, Ettlingen, Germany) equipped with an integrating sphere and operating in reflectance mode. The spectra were obtained at 64 scans with a resolution of 4 cm^{-1} and a spectral range of 10000-4000 cm^{-1} using the Opus program version 6.5 (Bruker Optics, Ettlingen, Germany).

Spectral analyses

The obtained data were processed using the chemometric program Unscrambler 10.1(AspenTech, Bedford, United States). Principal component analysis (PCA) was used to analyze the score and loading graphs to verify the differences between species based on the nonlinear iterative partial least squares (NIPALS) algorithm and cross validation with centered data. For the PCA through the NIR spectra, light scattering correction (MSC) was used, together with the first derivative of the Savitzky-Golay using 6 points and a second-order polynomial for the smoothing. The PCA through the VIS spectra used only MSC correction. For the NIR spectra, three principal components were applied to explain the variation in the data, while two were utilized for the VIS spectra.

The samples were randomly divided, with 75 % of the spectra were used for calibration and 25 % were used for external prediction. Spectral analysis was based on ASTM E1655-17 (2017).

Partial least squares regression (PLS-R) was applied to generate models for predicting the energy properties. The absorbance spectra acquired from the samples was correlated with

the values found in the laboratory tests by PLS regression. The samples were randomly divided using the same allocation as above. The spectral analysis was based on ASTM E1655-17 (2017). The models were built using the cross-validation method, with data centered on the mean and the NIPALS algorithm. The models were generated from the pre-treated spectra using MSC.

For the NIR spectra, three latent variables were used for the models of VMC, FCC, and AC, and two for the HHV. In the PLS-R models through the VIS spectra, two latent variables were used for all the analyzed properties.

The best prediction models were selected based on the following criteria: standard error of calibration (SEC), square error of validation (SEV), correlation of validation (R^2), and calibration, ratio of prediction deviation (RPD). The RPD represents the ratio between the standard deviation of the property values analyzed by the conventional method (SD) and the standard error of validation (SEV), obtained through the calibration models. This value allows the comparison between calibrations for different variables, since it enables the standardization of the standard error of the prediction (Williams and Sobering 1993).

Results and discussion

Wood energy properties

For energy production, a biomass with a high FCC and low VMC and AC values is required, as these conditions provide higher HHV per unit mass and greater thermal

stability. Therefore, the HHV is positively proportional to the FCC and negatively proportional to the VMC and AC (McKendry 2002). The studied species presented the typical energetic properties for wood previously reported, but with clear distinctions (Table 1). The wood of *Eucalyptus benthamii* is considered the most promising for energetic purposes, because it has the highest HHV and FCC, and the lowest VMC, despite a higher AC. The wood of *Eucalyptus dunnii* presented lower HHV and FCC values, a higher VMC, and an AC that was statistically as high as that of *Eucalyptus benthamii*. Finally, the wood of *Eucalyptus saligna* presented intermediate energetic properties to the two other species.

Table 1: Energetic properties of *E. benthamii*, *E. dunnii*, and *E. saligna* woods.

Species	VMC (%)	AC (%)	FCC (%)	HHV (kcal kg^{-1})
E. benthamii	79,84 c (0,37)	0,47 a (0,04)	19,68 a (0,38)	4378,17 a (91,50)
E. dunnii	82,42 a (0,54)	0,42 a (0,06)	17,16 c (0,52)	4252,50 b (65,48)
E. saligna	81,06 b (0,53)	0,31 b (0,07)	18,62 b (0,49)	4290,33 ab (34,47)

VMC: volatile material content (%), AC: ash content (%), FCC: fixed carbon content (%), HHV: higher heating value (kcal kg^{-1}).
Averages followed by the same lower-case letter in the same column are statistically equal using Tukey's test at 5 % probability.
Values in parentheses refer to standard deviation.

VIS spectroscopy

Figure 1 shows the score plot of principal components 1 and 2. Through the analysis of principal components, it was possible to observe the formation of three groups formed by

the three different eucalyptus species (Figure 1). Since all the woods were separated by both PC-1 and PC-2, only one principal component was sufficient to discriminate the three eucalyptus species. The two principal components together accounted for 99 % of the variability of the analyzed data, with 98 % explained by PC-1 and 1% by PC-2. As it can be observed in the PCA score plot (Figure 1), the positive scores on PC-1 are related for samples *Eucalyptus benthamii* specie and PC-1 negative values to *Eucalyptus saligna* and *Eucalyptus dunnii* samples.

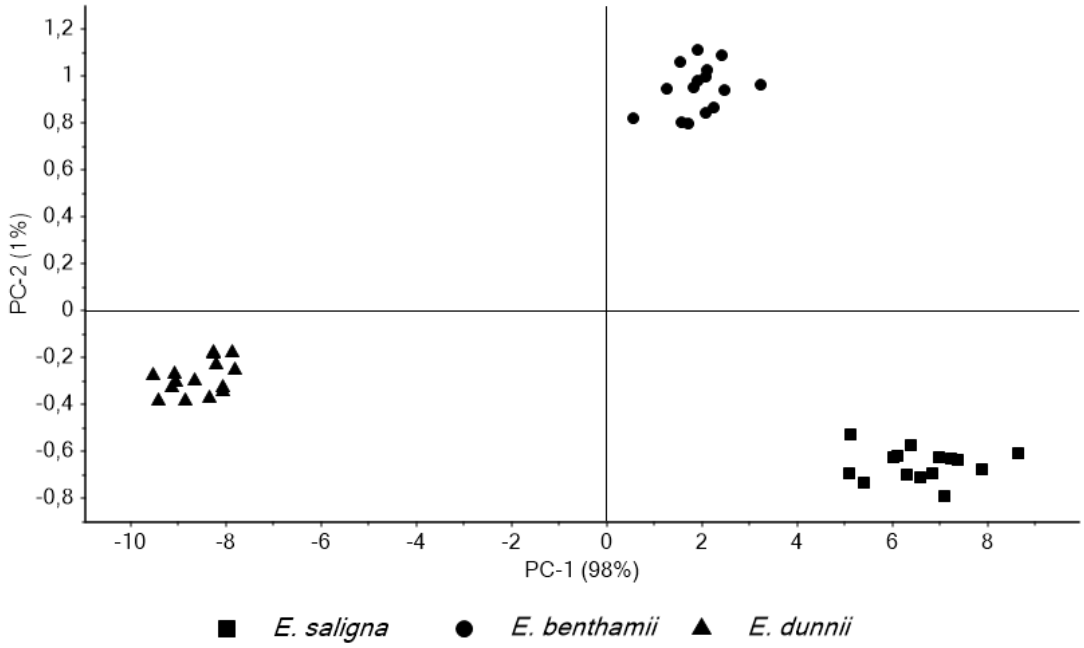

Figure 1: Two-dimensional scatter plot of the first and second principal components of the PCA scores.

Figure 2 represents the loading graph of the first two principal components (PCs) obtained by PCA of the VIS. The loading graph allowed evaluating the main wavelengths that most contributed to the separation of species. The highest absolute values of loading have a greater influence of this variable in the separation of samples, whether positive or

negative. Figure 2 shows the importance of the violet (380-440 nm), green (500-565 nm), yellow (590-625 nm), and red (625-740 nm) regions for species separation.

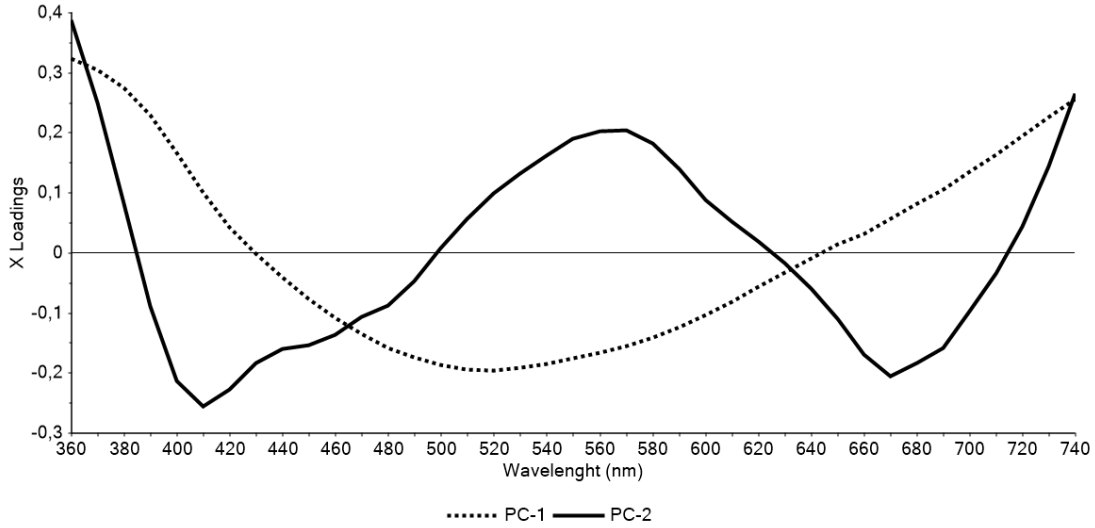

Figure 2: Loading graph for PCA analysis with vis.

Table 2 shows the principal parameters generated by the PLS-R calibration model using VIS spectroscopy.

Table 2: PLS-R model for wood energetic properties prediction by VIS spectra.

	VIS	VMC	AC	FCC	HHV
Calibration	SEC (error)	0,130	0,006	0,127	0,501
	RPD	3,498	7,936	3,540	130,724
	R^2	0,985	0,991	0,985	0,988
Validation	SEV (error)	0,146	0,022	0,106	0,658
	RPD	3,032	3,448	2,118	99,507
	R^2	0,976	0,966	0,977	0,985

VIS: visible spectroscopy, VMC: volatile material content, AC: ash content, FCC: fixed carbon content, HHV: higher heating value.

The square calibration error (SEC) was calculated using the samples for the model generated through the destructively obtained spectra and results, and the square validation

error (SEV) was the prediction error generated from the independent validation of this model. The ratio of prediction deviation (RPD) corresponds to the ratio between the standard deviation of the property values analyzed by the conventional method (SD) and the standard error of validation (SEV), obtained through the calibration models (Williams and Sobering 1993), which was used to evaluate the accuracy of the calibration performed and to compare the models. The coefficient of determination (R^2) showed the extent to which the values obtained by calibration or validation explained the values returned by the destructive analyses. R^2 values that are closer to 1 are desired.

The RPD is the main parameter that determines whether the model is satisfactory. In analytical chemistry, RPD values between 2 and 3 are considered sufficient for approximate predictions, those between 3 and 5 are satisfactory for prediction, and values greater than 5 indicate that the model can be used for quality control (Williams and Sobering 1993); however, in forest areas, a RPD greater than 1,5 is considered sufficient (Schimleck *et al.* 2003). For a model to be properly adjusted, the validation set must produce an SEV value like that of the SEC. SEV values excessively higher than the SEC indicate over-adjusted models, that is, the regression considers data that are not actually correlated, such as noise and other systematic errors (Ferrão *et al.* 2004).

It can be considered that all RPD values are high, especially for HHV prediction, and the difference between SEV and SEC in the HHV prediction model was greater than that of the other properties evaluated; however, all R^2 values were close to 1. These results identify the potential of using VIS for wood energy property prediction.

Table 3 shows the mean values and the coefficients of variation of the energy properties determined by the PLS-R of the VIS.

Table 3: Average values and standard deviations of energy properties predicted by PLS-R of VIS.

Species	VMC (%)	AC (%)	FCC (%)	HHV (kcal kg^{-1})
E. benthamii	79,84 (0,1683)	0,47 (0,0078)	19,68 (0,1496)	4363,37 (0,6519)
E. dunnii	82,31 (0,1161)	0,41 (0,0054)	17,27 (0,1037)	4355,24 (0,4432)
E. saligna	80,94 (0,4227)	0,33 (0,0197)	18,73 (0,3744)	4364,80 (1,6114)

VMC: volatile material content (%), AC: ash content (%), FCC: fixed carbon content (%), HHV: higher heating value (kcal kg^{-1}).
Values in parentheses refer to standard deviations.

The predicted values are close to those determined by destructive analysis, corroborating the strong performance of the PLS-R parameters (SEC, SEV, RPD, and R^2). However, the difference between the HHV values decreased, and the values found were closer to those of *Eucalyptus benthamii*. For all other properties, the predicted results were like the results obtained from the destructive tests, and the differences between the three species were maintained. The deficiency in the model to predict the HHV values can be attributed to the greater difference found between SEC and SEV when generating the models for this property.

NIR spectroscopy

Figure 3 shows the score plot of principal components 1 and 2. Using PCA (Figure 3), *Eucalyptus dunnii* was separated from the other species by PC-1, while *Eucalyptus benthamii* and *Eucalyptus saligna* were like each other but separated by the distance of the projection in PC-2. PC-1 explained 64% of the spectral variance and PC-2 described 9%, together accounting for 73% of the variability of the analyzed data. As it can be observed the samples of *E. benthamii* species are in the positive part of the PC1 while the

samples of the *Eucalyptus saligna* species are in the negative part. The negative scores of the *Eucalyptus benthamii* samples, indicate an inverse relationship with some chemical characteristic of the wood found in the *Eucalyptus saligna* samples (positive scores) used in the differentiation of the species. A third PC was performed, but no separation of the species occurred. In comparison with VIS PCA, which explained 99% of the spectral data in PC-1 and PC-2, the NIR spectra were more heterogeneous.

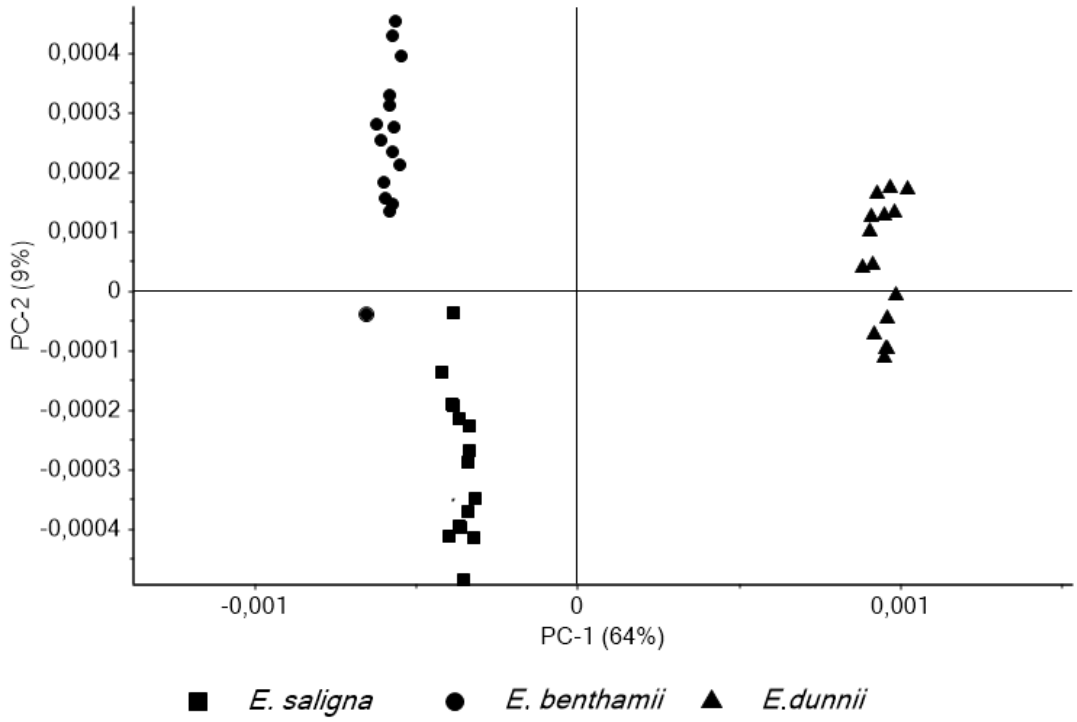

Figure 3: Two-dimensional scatter plot of the first and second principal components of the PCA scores.

Figure 4 presents the loading graph of the first two principal components (PCs) obtained by PCA. The loading graph allows identifying the vibrational peaks and bands that best contribute to the separation of classes. For the NIRS, the separation of the samples through the principal components occurred due to the difference in absorption at certain

wavelengths, and the most relevant peaks are presented in the loading graph of NIRS PCA (Figure 4). Table 4 shows the respective assignments of the vibrations of those peaks and the participation of the wood chemical components in the PCA analysis. The curves for PC-1 and PC-2 were highlighted because they were of greater relevance in the separation of the three studied species.

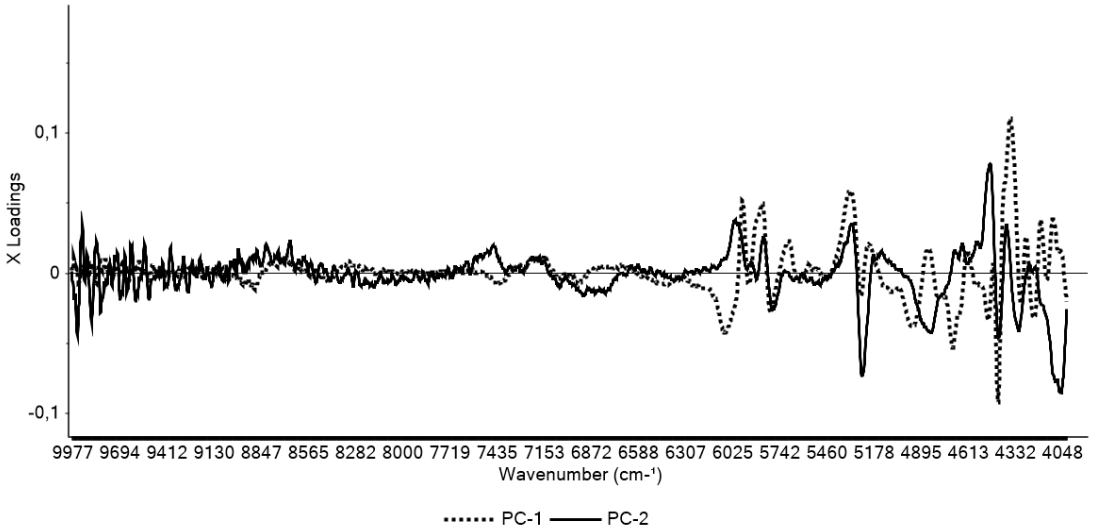

Figure 4: Loading graph for PCA analysis for NIRS.

Table 4: NIRS band attribution according to Siesler *et al.* (2002), Tsuchikawa and Siesler (2003), Schwanninger *et al.* (2011); and Chang *et al.* (2020).

Peak (cm^{-1})	Wood chemistry component	Bond vibration
6062	Hemicelluloses	C-H str
6003	Hemicelluloses	C-H str
5963	Lignin	C_{ar}-H str
5838	All components	C-H str
5327	Unidentified	C-H str
5250	Unidentified	C-H str
4476	Cellulose	O-H str + C-H str
4435	All components	O-H str + C-O str
4365	Cellulose	C-O str + O-H str or C-H_2 bend + C-H_2 str
4063	Carbohydrates	C-H str + C-C str

str: stretching vibration; ar: Aryl; and bend: bending vibration.

The relationship between the NIR spectra and chemical structures can aid in the interpretation of the PCA (Schwanninger *et al.* 2011); however, this relationship is also a weakness of NIRS due to spectral overlap, which commonly occurs when analyzing samples of complex chemical compositions and similar structures, such as those of natural compounds (Ma *et al.* 2019). The most relevant peaks to separate the three species occurred between 6062 and 4063 cm^{-1}, and all the chemical components of the wood were included in the species discrimination by PCA.

Table 5 shows the main parameters generated by the PLS-R calibration model using NIR spectroscopy.

Table 5: PLS-R model for wood energy properties prediction by NIRS.

	NIRS	VMC	AC	FCC	HHV
Calibration	SEC (error)	0,129	0,015	0,117	0,484
	RPD	3,508	3,268	3,836	135,479
	R^2	0,985	0,949	0,987	0,988
Validation	SEV (error)	0,146	0,022	0,106	0,658
	RPD	3,100	2,222	4,261	99,612
	R^2	0,9859	0,8968	0,9892	0,9779

NIRS: near-infrared spectroscopy, VMC: volatile material content, AC: ash content, FCC: fixed carbon content, HHV: higher heating value.

All the models generated by PLS-R through the NIR spectra for predicting the energy properties of the eucalyptus species were satisfactory, because, for both calibration and validation, the correlation coefficient (R^2) was close to 1, the error was close to zero, and the RPD was above 1,5 for all the studied properties.

All RPD values were considered high, especially HHV prediction, as reported in VIS, and SEV was considerably higher than SEC in the models for VMC and AC predictions. Like VIS, these results show the potential for using NIRS in the prediction of energetic wood properties.

The charcoal fixed carbon content (FCC) is directly related to the lignin and extractive contents and inversely to the holocellulose content. Compounds with a high carbon content, such as lignin and certain extractives of a phenolic nature, can contribute to increasing the higher heating value (HHV).

In the prediction of VMC, FCC, and HHV by NIRS of residues from the mechanical processing of tropical wood, Silva *et al.* (2014) found R^2 values as high as those of the present work, as well as satisfactory errors (SEC and SEV).

Andrade *et al.* (2012) used the partial least square (PLS) regressions to estimate fixed-carbon, volatile matter content and gravimetric yield of eucalyptus charcoal and obtained calibration coefficients in cross validation between 0,76 and 0,91.

Mancini and Rinnan (2021) analyzed waste wood samples from big panel board company by means of Near Infrared Spectroscopy. Principal Component Analysis has been used to investigate the variability of the material, and Partial-Least Squares regression models have been developed for the prediction of moisture content and net calorific value.

Table 6 shows the mean values and coefficients of variation of the energy properties determined by the PLS-R of NIRS.

Table 6: Average values and standard deviations of energy properties predicted by PLS-R of NIRS.

Species	VMC (%)	AC (%)	FCC (%)	HHV (kcal kg^{-1})
E. benthamii	79,95 (0,1223)	0,45 (0,0149)	19,59 (0,1269)	4363,57 (0,4286)
E. dunnii	82,44 (0,1415)	0,42 (0,0173)	17,13 (0,1472)	4354,32 (0,4258)
E. saligna	81,05 (0,1098)	0,33 (0,0134)	18,63 (0,1133)	4364,37 (0,3434)

VMC: volatile material content (%), AC: ash content (%), FCC: fixed carbon content (%), HHV: higher heating value (kcal kg^{-1}).
Values in parentheses refer to standard deviations.

The results predicted by NIRS had the same behavior as those obtained by using VIS, in that they were satisfactory values that decreased the differences between the species studied for HHV, and the values of this property were closer to those of *Eucalyptus benthamii* wood. The similarities between the predicted values and the values obtained using a destructive method for the other energetic properties of wood were also maintained.

Conclusions

The three *Eucalyptus* species presented distinct energetic properties. *Eucalyptus benthamii* revealed a higher HHV and FCC, while *Eucalyptus dunnii* displayed a lower HHV and FCC, and *Eucalyptus saligna* presented intermediate characteristics to those of the other species, along with a with lower AC.

PCA carried out for species discrimination was efficient, explaining 99% of the variance of the VIS spectra and 73 % of that of the NIR spectra, and VIS spectroscopy was considered the most suitable for discriminating species.

VIS and NIR spectroscopy associated with multivariate analysis has the potential to accurately estimate the main energetic properties of wood, and these technologies can be useful for industries that use wood as fuel, since all the models generated through the partial least square regression were satisfactory. The only differences observed between the techniques were the R^2 of the calibration and the validation of AC by NIRS, which were considerably lower than those determined by VIS. The spectroscopies studied in this

work allow real-time analysis, proving to be an adequate tool for product quality control and decision-making in the productive process of industries.

Authorship contributions

F.G.: Resources, data curation, investigation, methodology, validation. L.J.A.: Resources, data curation, investigation, methodology, validation. E.A.B.J.: Conceptualization, supervision, funding acquisition, writing – original draft. E.C.L.: Visualization, methodology, project administration, software, writing – review & editing. R.S.O.: Data curation, investigation. D.A.S.: Data curation, investigation, S.N.: Resources, methodology. L.C.V.: Methodology, visualization, writing – review & editing. D.M.S.: Investigation, visualization.

References:

Amaral, E.A.; Santos, L.M.; Costa, E.V.S.; Trugilho, P.F.; Hein, P.R.G. 2020. Estimation of moisture in wood chips by Near Infrared Spectroscopy. *Maderas. Ciencia y Tecnología* 22:291-302. https://doi.org/10.4067/S0718-221X2020005000304

ASTM. 2013. Standard Test Method for Gross Calorific Value of Coal and Coke. ASTM D5865-13. ASTM: West Conshohocken, PA, USA.

ASTM. 2017. Standard Practices for Infrared Multivariate Quantitative Analysis. ASTM E1655-17. ASTM: West Conshohocken, PA, USA.

ASTM. 2019. Standard Test Method for Analysis of Wood Fuels. ASTM E870-82. ASTM: West Conshohocken, PA, USA.

ASTM. 2019. Standard Test Method for Volatile Matter in the Analysis of Particulate Wood Fuels. ASTM E872-82. ASTM: West Conshohocken, PA, USA.

ASTM. 2021. Standard Test Method for Ash in Wood. ASTM D1102-84. ASTM: West Conshohocken, PA, USA.

Andrade, C.R.; Trugilho, P.F.; Hein, P.R.G.; Lima, J.T.; Napoli, A. 2012. Near infrared spectroscopy for estimating eucalyptus charcoal properties. *Journal of Near Infrared Spectroscopy* 20:657-666. https://doi.org/10.1255/jnirs.1028

Bersch, A.P.; Brun, E.J.; Pereira, F.A.; Silva, D.A.; De Barba, Y.R.; Dorini Junior, J.R. 2018. Characterization energy of wood of three genetic materials of *Eucalyptus* sp. *Floresta* 48(1):87-92. https://doi.org/10.5380/rf.v48i1.51673

Bonfatti Júnior, E.A.; Lengowski, E.C.; Takahashi, V.M.; Adur, G.M.; Silva, D.A.; Klock, U.; De Andrade, A.S.; Venson, I.; de Muñiz, G.I.B. 2019. Briquetting of

waste from mechanical and chemical processes of *Pinus* spp. *Cadernos de Ciencia & Tecnologia* 36:e26522. https://doi.org/10.35977/0104-1096.cct2019.v36.26522
Casson, A.; Beghi, R.; Giovenzana, V.; Fiorindo, I.; Tugnolo, A.; Guidetti, R. 2020. Environmental advantages of visible and near infrared spectroscopy for the prediction of intact olive ripeness. *Biosystems Engineering* 189:1-10. https://doi.org/10.1016/j.biosystemseng.2019.11.003
Chang, S.; Yin, C.; Liang, S.; Lu, M.; Wang, P.; Li, Z. 2020. Confirmation of brand identification in infant formulas by using near-infrared spectroscopy fingerprints. *Analytical Methods* 12:2469-2475. https://doi.org/10.1039/D0AY00375A
Chen, J.; Li, G. 2020. Prediction of moisture content of wood using Modified Random Frog and Vis-NIR hyperspectral imaging. *Infrared Physics & Technology* 105: e103225. https://doi.org/10.1016/j.infrared.2020.103225
Cortez, L.A.B.; Loura, E. S.; Gómes, E.O. 2014. Biomassa para bioenergia. 3rd ed. Campinas: UNICAMP.
Costa Junior, S.; Silva, D.A.; Behling, A.; Koehler, H.S.; Simon, A.A.; Costa, A. 2021. Propriedades energéticas da biomassa de *Acacia mearnsii* De Wild. em diferentes idades e locais de cultivo. *Scientia Forestalis* 49(131): e3406. https://doi.org/10.18671/scifor.v49n131.04
Cunha, C.L.; Torres, A.R.; Luna, A.S. 2020. Multivariate regression models obtained from near-infrared spectroscopy data for prediction of the physical properties of biodiesel and its blends. *Fuel* 261:e116344. https://doi.org/10.1016/j.fuel.2019.116344
de Abreu Neto, R.; Ramalho, F.M.G.; Costa, L.R.; Hein, P.R.G. 2020. Estimating hardness and density of wood and charcoal by near-infrared spectroscopy. *Wood Science and Technology* 55: 215-230. https://doi.org/10.1007/s00226-020-01232-y
Douglas, R.K.; Nawar, S.; Alamar, M.C.; Mouazen, A.M.; Coulon, F. 2018. Rapid prediction of total petroleum hydrocarbons concentration in contaminated soil using vis-NIR spectroscopy and regression techniques. *Science of The Total Environment* (616-617):147-155. https://doi.org/10.1016/j.scitotenv.2017.10.323
Friedl, A.; Padouvas, E.; Rotter, H.; Varmuza, K. 2005. Prediction of heating values of biomass fuel from elemental composition. *Analytica Chimica Acta* 544: 191-198. https://doi.org/10.1016/j.aca.2005.01.041
Fernandes, D.D.S.; Gomes, A.A.; Costa, G.B. da; da Silva, G.W.B.; Véras, G. 2011. Determination of biodiesel content in biodiesel/diesel blends using NIR and visible spectroscopy with variable selection. *Talanta* 87:30-34. https://doi.org/10.1016/j.talanta.2011.09.025
Ferrão, M.F.; Carvalho, C.W.; Müller, E.I.; Davanzo, C.U. 2004. Simultaneous determination of ash content and protein in wheat flour using infrared reflection techniques and partial least-squares regression (PLS). *Food Science and Technology* 24:333-340. https://doi.org/10.1590/S0101-20612004000300005
Garcia-Maraver, A.; Mata-Sanchez, J.; Carpio, M.; Perez-Jimenez, J.A. 2017. Critical review of predictive coefficients for biomass ash deposition tendency. *Journal of the Energy Institute* 90:214-228. https://doi.org/10.1016/j.joei.2016.02.002
Kobori, H.; Gorretta, N.; Rabatel, G.; Bellon-Maurel, V.; Chaix, G.; Roger, J.M.; Tsuchikawa, S. 2013. Applicability of Vis-NIR hyperspectral imaging for monitoring wood moisture content (MC). *Holzforschung* 67:307-314. https://doi.org/10.1515/hf-2012-0054
Kobori, H.; Kojima, M.; Yamamoto, H.; Sasaki, Y.; Yamaji, F.M.; Tsuchikawa, S. 2013. Vis-NIR spectroscopy for the on-site prediction of wood properties. *The Forestry Chronicle* 89: 631-638. https://doi.org/10.5558/tfc2013-114
Lana, A.Q.; Salles, T.T.; Carneiro, A. de C.O.; Cardoso, M.T.; Teixeira, R.U. 2016.

Comparison of procedures for immediate chemical analysis of charcoal. *Revista Árvore* 40:371-376. https://doi.org/10.1590/0100-67622016000200020
Lengowski, E.C.; Muñiz, G.I.B. de; Klock, U.; Nisgoski, S. 2018. Potential use of nir and visible spectroscopy to analyze chemical properties of thermally treated wood. *Maderas. Ciencia y Tecnología* 20: 627-640. https://doi.org/10.4067/S0718-221X2018005041001
Liu, Z.; Fei, B.; Jiang, Z.; Cai, Z.; Liu, X. 2014. Important properties of bamboo pellets to be used as commercial solid fuel in China. *Wood Science and Technology* 48:903-917. https://doi.org/10.1007/s00226-014-0648-x
Li, Y.; Via, B.K.; Li, Y. 2020. Lifting wavelet transform for Vis-NIR spectral data optimization to predict wood density. *Spectrochimica Acta Part A: Molecular and Biomolecular Spectroscopy* 240: e118566. https://doi.org/10.1016/j.saa.2020.118566
Li, Y.; Via, B.; Cheng, Q.; Li, Y. 2018. Lifting Wavelet Transform De-noising for Model Optimization of Vis-NIR Spectroscopy to Predict Wood Tracheid Length in Trees. *Sensors* 18(12): e4306. https://doi.org/10.3390/s18124306
Llana, D.F.; Íñiguez-González, G.; Díez, M.R.; Arriaga, F. 2020. Nondestructive testing used on timber in Spain: A literature review. *Maderas. Ciencia y Tecnología* 22:133-156. https://doi.org/10.4067/S0718-221X2020005000201
Loureiro, B.A.; Assis, M.R.de; Melo, I.C.N.A. de; Oliveira, A.F.F. de; Trugilho, P. F. 2021. Rendimento gravimétrico da carbonização e caracterização qualitativa do carvão vegetal em clones de híbridos de *Corymbia* spp para uso industrial. Ciênc. *Ciência Florestal* 31(1): 214-232. https://doi.org/10.5902/1980509836120
Ma, L.; Peng, Y.; Pei, Y.; Zeng, J.; Shen, H.; Cao, J.; Qiao, Y.; Wu, Z. 2019. Systematic discovery about NIR spectral assignment from chemical structural property to natural chemical compounds. *Scientific Reports* 9: e9503. https://doi.org/10.1038/s41598-019-45945-y
Mancini, M.; Rinnan, **Å. 2021.** Near infrared technique as a tool for the rapid assessment of waste wood quality for energy applications. *Renewable Energy* 177:113-123. https://doi.org/10.1016/j.renene.2021.05.137
McKendry, P. 2002. Energy production from biomass (part 1): Overview of biomass. *Bioresource Technology* 83:37-46. https://doi.org/10.1016/S0960-8524(01)00118-3
Nisgoski, S.; Muñiz, G.I.B. de; Gonçalves, T.; Ballarin, A. 2017. Use of visible and near-infrared spectroscopy for discrimination of eucalypt species by examination of solid samples. *Journal of Tropical Forest Science* 29:371-379 https://www.jstor.org/stable/44272915
Orellana, B.B.M.A.; Vale, A.T. do; Orellana, J.B.P.; Chaves, B.S.; Moreira, A.C. de O. 2020. Characterization of agricultural residues from Federal District region for energy purposes. *Energia na Agricultura* 35:46-61. https://doi.org/10.17224/EnergAgric.2020v35n1p46-61
Oliveira, M.G. de; Christoforo, A.L.; Araujo, V.A.; Lahr, F.A.R. 2016. Química da Madeira no Contexto Energético. São Carlos: EESC/USP. https://www.researchgate.net/profile/Francisco-Rocco-Lahr/publication/308890980_Quimica_da_Madeira_no_Contexto_Energetico/links/57f52d4308ae280dd0b8d98d/Quimica-da-Madeira-no-Contexto-Energetico.pdf
Pádua, F.A. de; Tomeleri, J.O.P.; Franco, M.P.; Silva, J.R.M. da; Trugilho, P.F. 2019. Recommendation of non-destructive sampling method for density estimation of the *Eucalyptus* wood. *Maderas. Ciencia y Tecnología* 21:565-572. https://doi.org/10.4067/S0718-221X2019005000412
Pilar Dorado, M.; Pinzi, S.; de Haro, A.; Font, R.; Garcia-Olmo, J. 2011. Visible and NIR Spectroscopy to assess biodiesel quality: Determination of alcohol and

glycerol traces. *Fuel* 90: 2321-2325. https://doi.org/10.1016/j.fuel.2011.02.015
Pincelli, A.L.P.S.M.; Queiroz, I.S. de. 2021. Parâmetros físico-químicos de diferentes resíduos agroindustriais para fins energéticos. *Bioenergia em Revista Diálogos* 11(2): 52-68.
http://fatecpiracicaba.edu.br/revista/index.php/bioenergiaemrevista/article/view/441
Preece, S.L.M.; Auvermann, B.W.; MacDonald, J.C.; Morgan, C.L.S. 2013. Predicting the heating value of solid manure with visible and near-infrared spectroscopy. *Fuel* 106:712-717. https://doi.org/10.1016/j.fuel.2012.10.006
Rumble, J.R. 2020. *CRC Handbook of Chemistry and Physics*. 101st ed. Boca Raton: CRC Press.
Santos, F.D.; Santos, L.P.; Cunha, P.H.P.; Borghi, F.T.; Romão, W.; de Castro, E.V.R.; de Oliveira, E.C.; Filguerias, P.R. 2021. Discrimination of oils and fuels using a portable NIR spectrometer. *Fuel* 283: e118854. https://doi.org/10.1016/j.fuel.2020.118854
Shen, J.; Zhu, S.; Liu, X.; Zhang, H.; Tan, J. 2010. The prediction of elemental composition of biomass based on proximate analysis. *Energy Conversion and Management* 51: 983-987. https://doi.org/10.1016/j.enconman.2009.11.039
Schimleck, L.R.; Mora, C.; Daniels, R.F. 2003. Estimation of the physical wood properties of green *Pinus taeda* radial samples by near infrared spectroscopy. *Canadian Journal of Forest Research* 33:2297-2305. https://doi.org/10.1139/x03-173
Schwanninger, M.; Rodrigues, J.C.; Fackler, K. 2011. A review of band assignments in near infrared spectra of wood and wood components. *Journal of Near Infrared Spectroscopy* 19: 287-308. https://doi.org/10.1255/jnirs.955
Silva, D.A. da; Almeida, V.C.; Viana, L.C.; Klock, U.; Muñiz, G.I.B. de. 2014. Avaliação das propriedades energéticas de resíduos de madeiras tropicais com uso da espectroscopia NIR. *Floresta e Ambiente* 21:561-568. https://doi.org/10.1590/2179-8087.043414
Siesler, R.W.; Ozaki, Y.; Kawata, S.; Heise, H.M. 2002. Near infrared spectroscopy: principles, instruments, applications. New York: Wiley.
TAPPI. 2021. Sampling and preparing wood for analysis. TAPPI T257 sp-21. TAPPI Standard Method: Atlanta, USA.
https://imisrise.tappi.org/TAPPI/Products/01/T/0104T257.aspx
Telmo, C.; Lousada, J. 2011. The explained variation by lignin and extractive contents on higher heating value of wood. *Biomass and Bioenergy* 35:1663-1667. https://doi.org/10.1016/j.biombioe.2010.12.038
Tsuchikawa, S.; Siesler, H.W. 2003. Near-infrared spectroscopic monitoring of the diffusion process of deuterium-labeled molecules in wood. Part I: Softwood. *Applied Spectroscopy* 57:667-674. https://doi.org/10.1366/000370203322005364
Vassilev, S.V.; Vassileva, C.G. 2020. Contents and associations of rare earth elements and yttrium in biomass ashes. *Fuel* 262: e116525. https://doi.org/10.1016/j.fuel.2019.116525
Williams, P.C.; Sobering, D.C. 1993. Comparison of commercial near infrared transmittance and reflectance instruments for analysis of whole grains and seeds. *Journal of Near Infrared Spectroscopy* 1: 25-32. https://doi.org/10.1255/jnirs.3